Science of the Total Environment 800 (2021) 149556

Contents lists available at ScienceDirect

Science of the Total Environment

journal homepage: www.elsevier.com/locate/scitotenv

Toxicity of lanthanide coagulants assessed using four in vitro bioassays

George William Kajjumba [a], Matias Attene-Ramos [b], Erica J. Marti [a,*]

[a] Department of Civil and Environmental Engineering and Construction, University of Nevada, Las Vegas, 4505 S. Maryland Pkwy., Las Vegas, NV 89154, USA
[b] Department of Environmental and Occupational Health, Milken Institute School of Public Health, George Washington University, DC, USA

HIGHLIGHTS

- Toxicity of lanthanides was evaluated using an array of *in vitro* mechanistic assays.
- Δψm is less affected by lanthanides compared to chronic toxicity and cell viability.
- Lanthanides exhibit antagonistic toxicity at less than 1000 μmol-Ln^{3+}/L.
- Lanthanides exhibited no sign of genotoxicity.

GRAPHICAL ABSTRACT

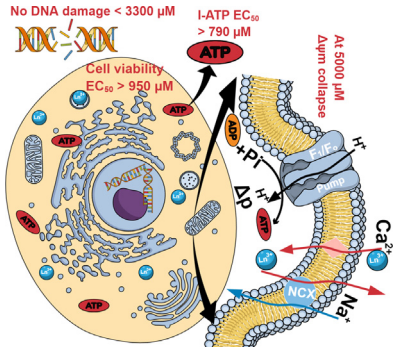

ARTICLE INFO

Article history:
Received 15 April 2021
Received in revised form 3 August 2021
Accepted 5 August 2021
Available online 9 August 2021

Editor: Henner Hollert

Keywords:
Mitochondrial membrane potential
Toxicity bioassay
Chronic toxicity
Genotoxicity
Toxicity additivity
Rare earth elements

ABSTRACT

Rare earth element (REE) coagulants are prime contenders in wastewater treatment plants to remove phosphorus; unlike typical coagulants, they are not affected by pH. However, the use of REEs in wastewater treatment could mean increased human exposure to lanthanides (Ln) through wastewater effluent discharge to the environment or through water reuse. Information on the toxicity of lanthanides is scarce and, where available, there are conflicting views. Using in vitro bioassays, we assessed lanthanide toxicity by evaluating four relevant endpoints: the change in mitochondrial membrane potential (Δψm), intracellular adenosine triphosphate (I-ATP), genotoxicity, and cell viability. At less than 5000 μmol-Ln^{3+}/L, lanthanides increased the Δψm, while above 5000 μmol-Ln^{3+}/L, the Δψm level plummeted. The measure of I-ATP indicated constant levels of ATP up to 250 μmol-Ln^{3+}/L, above which the I-ATP decreased steadily; the concentration of La, Ce, Gd, and Lu that triggered half of the cells to become ATP-inactive is 794, 1505, 1488, 1115 μmol-Ln^{3+}/L, respectively. Although La and Lu accelerated cell death in shorter studies (24 h), chronic studies using three cell growth cycles showed cell recovery. Lanthanides exhibited antagonistic toxicity at less than 1000 μmol-Ln^{3+}/L. However, the introduction of heavy REEs in a solution amplified lanthanide toxicity. Tested lanthanides appear to pose little risk, which could pave the way for lanthanide application in wastewater treatment.

1. Introduction

Processes like fertilizer application in agriculture, damaged septic systems and urban wastewater systems can cause elevated discharges of phosphorus into the hydrosphere. As low as 0.1 mg/L phosphorus is sufficient to initiate water pollution through eutrophication (Correll 1998), which can lead to algal blooms and oxygen depletion that cause fish death and resource loss (Abbas et al., 2020). Hence, there is a need to remove phosphorus from wastewater before it is discharged to water bodies. The use of lanthanide elements—namely lanthanum (La), cerium (Ce), gadolinium (Gd), and lutetium (Lu)—through coagulation and adsorption processes is a promising approach to remove and

* Corresponding author at: 4505 S. Maryland Pkwy, Las Vegas, NV 89154, USA.
E-mail addresses: gwkajjumba@gmail.com (G.W. Kajjumba), erica.marti@unlv.edu (E.J. Marti).

https://doi.org/10.1016/j.scitotenv.2021.149556
0048-9697/

retrieve phosphorus from wastewater (Kulperger et al., 2001; Recillas et al., 2012; Wang et al., 2016). However, this process would result in residual lanthanide concentrations in the wastewater effluent that is discharged to the environment. Through coagulation, 1.2 mol of Ln^{3+} are sufficient to precipitate 1.0 mol of phosphorus from wastewater leaving at most 0.5 mg Ln^{3+}/L effluent concentration (Kajjumba et al., 2021). Due to different anthropogenic activities (e.g. medical, electronics and energy industries), 1.0 ng Ln^{3+}/L to 10.0 μg Ln^{3+}/L has been detected in environmental water sources (Blinova et al., 2018; Herrmann et al., 2016; Weltje et al., 2002).

As policy makers mandate lower phosphorus effluent levels from wastewater treatment plants (WWTPs), treatment plants will seek out more efficient materials/chemicals like lanthanides. However, the application of lanthanides in WWTPs begs the question—"*are they introducing another toxic chromium*?" Toxicological studies of lanthanides are relatively scarce to date. At concentrations as low as 0.3-0.5 mg/L, lanthanides induced significant chronic toxicity in microcrustaceans (Blinova et al., 2018). The study of lanthanide toxicity with RAW264.7 cell line and HUCPV stem cells elicited that 148-372 mg/L was sufficient to inhibit cell function process to half (Feyerabend et al., 2010). Other studies have shown that lanthanides can affect the liver, brain, lungs, and blood, causing proinflammatory cytokines (Herrmann et al., 2016; Pagano et al., 2015). Nevertheless, little is understood about their mechanisms of toxicity.

Experimental studies in cell lines and bacteria are commonly used to quickly identify possible toxic substances and assess their possible mechanism of toxicity (Huang et al., 2008). Assays may assess one or more toxicity endpoint, such as carcinogenicity, ecotoxicity, genotoxicity and neurotoxicity, among others. In eukaryotic cells, mitochondria act as the powerhouse; shortage of adenosine triphosphate (ATP) can lead to cell death. Contaminants that can distort mitochondrial membrane potential could lead to the onset of many disorders, including cancer, diabetes, and neurodegenerative and cardiovascular diseases (Attene-Ramos et al., 2015; Lesnefsky et al., 2001; Pieczenik and Neustadt, 2007). Measuring cytotoxicity or cell viability provides a general view of a compound's toxicity, and multiple methods have been employed for rapid chemical screening, including ATP assays, resazurin or other dyes, and the lactate dehydrogenase assay. Various cell lines can be used in these bioassays with human hepatoma (HepG2), human breast cancer (MCF7) and human cervical carcinoma (HeLa) cells frequently employed. In water treatment, a dye-based test using Chinese hamster ovary (CHO) cells has been used to assess chronic toxicity of chemicals present in water samples (Plewa et al., 2010). Cells like HepG2 and CHO are suitable for in vitro studies because of their high degrees of morphological and functional differentiation (Shen et al., 2012).

The objectives of this study were to explore the toxic properties of lanthanides using a set of bioassays for cytotoxicity, genotoxicity, and mitochondrial activity and a range of concentrations that might be permitted/detected after lanthanide coagulant use in WWTPs. Specifically, we aimed to (i) measure the acute effect of lanthanides on mitochondrial membrane potential that could lead to mitochondrial dysfunction; (ii) explore the impact of lanthanides on intracellular ATP and cell viability; (iii) estimate lanthanide chronic toxicity by using a well-established CHO assay (Plewa et al., 2010), and (iv) evaluate whether lanthanides are genotoxic or not. To further understand the combined effect of lanthanides, different combinations of lanthanides were studied. In this study, La and Ce represented light lanthanides, while gadolinium and lutetium represented medium and heavy REEs, respectively. Furthermore, the tests presented here could offer guidance on developing lanthanide operation permits and bioanalytical monitoring tools in water quality assessment and monitoring.

2. Materials and methods

The HepG2 cells and Eagle's minimum essential medium (EMEM) were supplied by ATCC™ (Manassas, VA, USA). CHO cells were obtained from Dr. Michael Plewa's lab. F-12 and fetal bovine serum (FBS) were supplied by Gibco™ (Gaithersburg, MD), while penicillin-streptomycin solution, 200× signal enhancer, 10× buffer solution were supplied by HyClone™ (South Logan, UT, USA). Mitochondrial membrane potential indicator was obtained from Codex™ (Gaithersburg, MD, USA). The Cell Titer Blue® and CellTiter-Glo® cell viability assays were supplied by Promega (Madison, WI, USA). The umuC assay was supplied by EBPI™, Canada. Carbonyl cyanide-*p*-trifluoromethoxyphenylhydrazone (FCCP) was purchased from Sigma-Aldrich (St. Louis, MO, USA). Lanthanum chloride ($LaCl_3{\cdot}7H_2O$, CAS 10025-84-0, 99%), cerium chloride ($CeCl_3$, CAS 18618-55-8, 99%), gadolinium chloride ($GdCl_3$, CAS 13450-84-5, 99.9%), and lutetium chloride ($LuCl_3$, CAS 15230-79-2, 99.9%) were supplied by Alfa Aesar (MA, USA). ACS-grade sodium chloride (NaCl, CAS 7647-14-5) was purchased from Fisher Chemical.

2.1. Cell culture and treatment

The culturing of HepG2 cells is described elsewhere (Sakamuru et al., 2016). In summary, the cells are maintained in EMEM, a high glucose medium with glutamine. The EMEM solution was supplemented with 10% fetal bovine serum and 1.0% penicillin-streptomycin solution. The CHO cells were maintained in an F-12 nutrient mixture with glutamine, supplemented with 5.0% FBS and 1.0% penicillin-streptomycin solution. The cells were cultured in T-75 flasks in a humidified environment at 37 ± 0.5 °C and 5.0 ± 0.2% CO_2. After attaining 70% confluence, the cells were either seeded in well plates for assay preparation or subcultured to another flask; Fig. S1 shows the step-by-step preparation of assays.

2.2. Mitochondrial membrane potential

Mitochondrial membrane potential (Δψm) was determined using the Δψm indicator solution. Steps for preparation of Δψm indicator are summarized in the Supplementary Materials, Section 1.1 (Sakamuru et al., 2016). To each well of a 96-well black clear-bottom plate, 50 μL of 800,000 HepG2 cells/mL were seeded and incubated at 37 ± 0.5 °C in a 5 ± 0.2% CO_2 environment. At least 4 h after seeding, the medium was removed from each well, and each well was treated with 50 μL of the respective lanthanide concentration (treatment), FCCP (positive control) or medium (negative control). FCCP is a known mitochondrial inhibitor that has shown to be an effective positive control for this assay (Sakamuru et al., 2016). Lanthanide stock solutions were prepared in deionized water from which aliquots were taken and mixed with cell medium to create 50, 100, 250, 500, 1000, 2500, 5000, 8000, and 10,000 μM. It was ensured that the overall volume contribution of the aliquot was less than 0.5% (v/v) to prevent medium dilution. The plate was then incubated for 60 min before the addition of 50 μL of Δψm indicator solution, after which the plate was incubated for 30 min. The level of Δψm disruption was measured from the bottom of the plate at 485 nm and 535 nm (green fluorescence), and 540 nm and 590 nm (red fluorescence).

2.3. Intracellular ATP and cell viability

Intracellular ATP (I-ATP) studies were conducted in a 96-well opaque white plate while cell viability studies were conducted in a 96-well black clear-bottom plate. Each well, except for positive controls, was seeded with 50 μL of 800,000 HepG2 cells/mL. The plates were incubated at 37.0 ± 0.5 °C in a humidified environment of 5.0 ± 0.2% CO_2 for at least 4 h to allow the cells to attach. Sections 1.2 and 1.3 in the Supplementary Materials explain the process of measuring I-ATP and cell viability. Lanthanides were obtained with chloride ligands; therefore, NaCl was used as a control to determine the effect of chloride ions. For this assay, positive control wells did not have any HepG2 cells (i.e., wells contained medium only), while negative control wells had HepG2 cells and did not receive lanthanide treatment.

2.4. Chronic cytotoxicity assay

The effect of lanthanides on the growth of cells was studied with CHO cells. By measuring the number of viable cells after 72 h (3-4 cell cycles), chronic toxicity of a target contaminant can be established. To each well of a 96-well white clear-bottom plate, 100 μL of respective Ln concentration (50-10,000 μM) prepared in cell medium was added. This was followed by 100 μL of 30,000 cells/mL to all wells except for the positive controls. The wells were covered with an aluminum plate seal and incubated at 37 °C in a humidified environment with 5 ± 0.2% CO_2 for 72 h. After 72 h, the treatment was removed, and the cells were fixed with 50 μL of methanol for 10 min. The cells were stained with 50 μL of crystal violet solution for 10 min. After 10 min, the plate was washed in deionized water to remove the unabsorbed crystal violet. Then 50 μL of methanol-dimethyl sulfoxide solution (25:75 v/v) was added; the plate was kept in the dark for 10 min before measuring the absorbance at 595 nm (Attene-Ramos et al., 2006; Plewa et al., 2004). Wells without any CHO cells were used as a positive control, while untreated wells were used as a negative control. The assay detected 300 to 50,000 cells. CHO cell medium was prepared, as shown in Table S1, and crystal violet solution was prepared as indicated in Table S2.

2.5. Genotoxicity of REE

Genotoxicity was measured through β-galactosidase activity; *Salmonella typhimurium* bacteria TA1535/pSK1002 were used to produce β-galactosidase in a umu-Chromotest™ assay (EBPI, Canada). This assay provides an indirect approach for assessing genotoxicity through activation of the SOS pathway, which is a cellular response to DNA damage. The induction of SOS-DNA response is observed as a measurable colorimetric endpoint. The genotoxicity assay procedure was entirely based on the manufacturer's protocol (EBPI, Canada).

2.6. Additive, antagonistic, and synergistic (AAS) effects of lanthanides

The presence of more than one compound in a water matrix can cause a different effect as compared to an individual compound. The compounds can inhibit each other as they compete for the same active sites or show an increased response through synergistic effects. To understand the AAS nature of lanthanides, we used the Chou-Talalay model (CT model) to estimate combination indexes (CI) (Chou, 2010). The CT model combines the Hill, Henderson-Hasselbalch, Michaelis-Menten, and Scatchard equations to develop a robust model that can predict the combined effect of drugs/contaminants. Fig. S2 explains the step-by-step process of the CT model. When CI < 0.9, the combined impact of lanthanides is synergistic in nature, while 0.9 ≤ CI ≤ 1.1 represents an additive effect and CI > 1.1 signifies an antagonistic effect among lanthanides.

2.7. Data analysis

The Δψm, I-ATP, chronic toxicity, and cell viability were determined as an average reduction in cell activity after exposure to lanthanide solution as compared to the negative control (untreated). The ratio of viable cells was calculated with Eq. (1). Here, A_s is the absorbance/fluorescence/luminescence (A/F/L) of a sample, B_{pc} is the A/F/L of the positive control (no-cell control or cells treated with FCCP for case of Δψm) used to eliminate the effect of background noise, and C_{NC} is the A/F/L of the negative control (i.e., untreated cells). At least two independent experiments were conducted for each assay, and the mean represents at least four data points. All results are presented as mean ± SD (standard deviation).

$$\Delta\psi m/I-ATP/\text{Cell viability}/\text{Chronic cytotoxicity response} = \frac{A_s - B_{pc}}{C_{NC} - B_{pc}} \quad (1)$$

2.8. Half-maximal response (EC_{50})

The half-maximal inhibitory concentration, EC_{50}, is a toxicity measure which indicates the concentration of a compound that is needed to inhibit a given biological process to half. A dose-response graph is used in which the effect of the target response is plotted as a function of compound concentration. The Hill equation is widely used to describe the growth-sigmoidal relationship; for this study, the dose-response model Eq. (2) was used.

$$EC = A_1 + \frac{A_2 - A_1}{1 + 10^{(\log EC_{50} - C)\alpha}} \quad (2)$$

Here, EC is the predicted effect of the lanthanide, A_1 is the minimum impact, A_2 is the maximum effect, C is the lanthanide concentration, log EC_{50} is the lanthanide concentration for which 50% of the maximum effect is obtained, and α is the Hill coefficient of sigmoidicity (Islami-Moghaddam et al., 2009).

3. Results and discussion

3.1. Mitochondrial membrane potential

Mitochondria are double-membrane organelles that harness the energy that cells need to grow and reproduce (Aldridge and Street, 1964). The inner mitochondrial membrane acts as a barrier to positively charged particles (protons, H^+), allowing a proton concentration gradient (Δp) between the matrix (fewer H^+) and intermembrane space (more H^+) (Mitchell and Moyle, 1969; Nicholls and Budd, 2000). Just as wind turbines use wind to generate energy, the F_1/F_0 complex (ATP synthase) is driven by the proton gradient to synthesize ATP as protons move from intermembrane space to the matrix. This process is maintained by Complexes I, II, III, and IV (Nicholls and Budd, 2000). The effect that lanthanides have on the Δψm was studied on HepG2 cells using a water-soluble Δψm indicator to measure changes in the Δψm as a proxy for function. The cells were exposed to lanthanide solution for 90 min to measure the acute mitochondrial effect while minimizing cell cytotoxicity (Attene-Ramos et al., 2015). When the cells are subjected to Δψm indicator dye, healthy cells accumulate the dye in the intermembrane space, emitting red fluorescence under 540 nm and 590 nm excitation. However, when the Δψm gets disrupted, the Δψm dye remains in the cytoplasm, emitting green fluorescence at 485 nm and 535 nm excitation energy. The ratio of red/green fluorescence determines the level of Δψm function compared to the control—untreated cells (Sakamuru et al., 2016).

Fig. 1 shows the response of HepG2 during the 1.5-h exposure to lanthanides. La, Ce, Gd, and Lu did not decrease the activity of mitochondria within the non-cytotoxic range (0-5000 μmol-Ln^{3+}/L); in fact, mitochondrial activity slightly increased with concentration. At 5000 μmol-Ln^{3+}/L, Ce, La, and Lu significantly increased the cell response up to 127.5 ± 11.9%, 139.7 ± 9.8%, and 138.3 ± 12.3% ($\rho < 0.05$), respectively. Gd showed the least increase in the membrane potential, 100.8 ± 29.7% ($\rho = 0.908$). Previously, Arya et al. (2014) showed that the treatment of cells with cerium nanoparticles (25 nM) followed by hydrogen peroxide (50 μM) increased the Δψm up to 129% compared to the control. Lanthanides could achieve this observation by restoring the balance between major redox reactions like NADH/NAD^+, leading to the accumulation of antiapoptotic proteins like myeloid cell leukemia-1 (Mcl-1) and B-cell lymphoma-2 (Bcl-2) (Arya et al., 2014; Hussain et al., 2016) or through sustained activation of focal adhesion kinase (FAK) (Zhang et al., 2009). Phosphorylation of FAK signaling improves cell adhesion, motility, and survival (Parsons, 2003; Slack et al., 2001) which in turn ameliorates Δψm to produce ATP necessary to sustain these processes. This data suggests that during water treatment with lanthanides, an effluent concentration close to 5000 μmol-Ln^{3+}/L should be avoided.

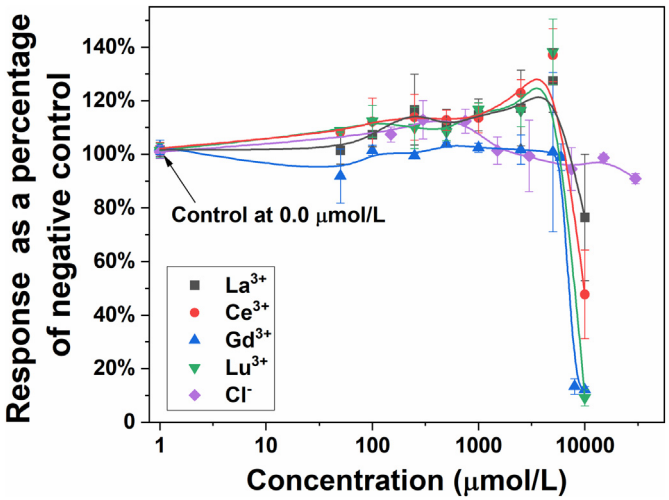

Fig. 1. The effect of La, Ce, Gd, and Lu on the Δψm of HepG2 cells. Duration = 1.5 h; cells per well = 80,000 cells/well; Ln^{3+} treatment volume per well = 100 μL; negative control = untreated cells; positive control = cells treated with FCCP at 2000 μM. The X-axis is on a $10^{\times}$ scale. Each data point represents the mean of at least two independent experiments and $n \geq 4$, and error bars show one standard deviation.

Above 5000 μmol-Ln^{3+}/L, regardless of the type of lanthanide, Δψm plummeted. The decrease could be associated with cell cytotoxicity; however, the mechanism is not clear. The decrease might not be attributed to caspase activation or production of reactive oxygen species (ROS) (Hussain et al., 2012) but rather to mitochondrial damage and excessive usage of ATP or phosphate precipitation by lanthanides. In addition, lanthanide regulation is assumed to be related to calcium regulation because of the similarity in ionic radius: 92-117 pm for lanthanides and 114 pm for calcium (Reeves and Condrescu, 2003). Lanthanides diffuse into the mitochondria using the Ca^{2+} channels. At low concentration, the calmodulin can regulate the excess lanthanides that enter the cell. As the concentration of lanthanides/Ca^{2+} increase, the sodium-calcium channel (NCX) is activated to pump out excess lanthanides/Ca^{2+} (Reeves and Condrescu, 2003; Wu et al., 2013). The NCX, orchestrated through the sodium-potassium pump, is an ATP-intensive process. The bioenergetic proton gradient (Δp) regulates ATP production, while the Δψm portion of Δp balances the Ca^{2+} gradient and ROS production (Perry et al., 2011; Szabadkai and Duchen, 2008). An excessive presence of lanthanides/Ca^{2+} increases pH and osmolality, altering Δp and thus ATP production. When lanthanide/Ca^{2+} flux surpasses the mitochondria's buffering ability, Δp, Δψm, and mitochondrial pH gradient (ΔpHm) are ultimately lost, diminishing ATP production and accelerating bioenergetic stress (Duchen, 2004). Therefore, at 5000 μmol-Ln^{3+}/L and above, lanthanides affect Δp, Δψm, and ΔpHm that might inhibit ATP production leading to cellular death.

Traditional coagulants that are used in wastewater treatment, like aluminum sulfate, elicit a similar trend. The study of Arab-Nozari et al. (2019) matched the levels of aluminum ions and nanoparticles in relation to Δψm. They reported an increase of Δψm for both aluminum species. Compared to the negative control, Δψm increased by over 23% at 200 μM of aluminum ions. However, in another study, at as low as 50 μM, aluminum triggered the mitochondria to release cytochrome C and decreased Bcl-2, causing mitochondrial mediated apoptosis (Kumar and Gill, 2014). The presence of iron, another prominent coagulant in wastewater treatment, accelerates the loss of Δψm through redox mechanism (Zhang et al., 2005). Therefore, lanthanides seem to be less toxic for mitochondria than aluminum and iron.

3.2. Intracellular ATP

A luminescence assay based on luciferase is a fast and simple method for determining ATP production and cell viability (Hannah et al., 2001). Luciferase, an enzyme derived from *Photuris pennsylvanica* or firefly, catalyzes the conversion of D-luciferin into oxyluciferin, and the result is luminescence. The process takes place in the presence of ATP, oxygen and magnesium ions (Tomasello et al., 2019); Fig. S3 summarizes the mechanism. CellTiter-Glo® (CTG) provides luciferin and luciferase necessary to produce luminescence; the intensity of the light that can be measured by a luminometer reflects the level of I-ATP (Riss et al., 2003). The main advantage of CTG is that it is less sensitive to pH and detergents compared to luciferase purified from *Photinus pyralis*. Besides, its luminescence has a half-life of over 5 h. CTG can detect luminescence due to ATP even as low as 15 cells within 10 min. Thus, CTG was applied to study the I-ATP of HepG2 cells.

Both La and Lu elicited a potent effect on I-ATP; at 1000 μmol-Ln^{3+}/L, more than half of the ATP was lost compared to the controls after 24 h (Fig. 2A). At 5000 μmol-Ln^{3+}/L, lanthanides attenuated ATP to less than 1.0% regardless of the compound, suggesting that most of the cells were dead at that concentration. Lanthanide chlorides were used in the study. To ensure that the loss of ATP was not due to the concentration of chloride ions, parallel experiments with NaCl were conducted. No significant I-ATP change was registered even at the highest tested concentration of 30,000 μmol-Cl^-/L (84.2 ± 13.4%). Thus, the ATP

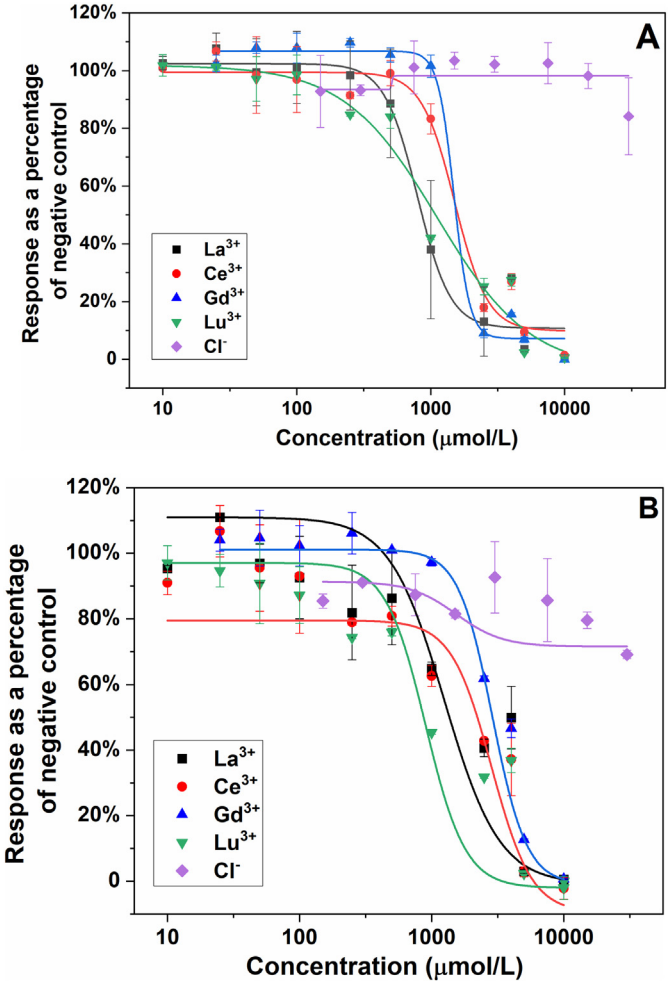

Fig. 2. Effect of lanthanides on (A) intracellular ATP measured with CellTiter-Glo® and (B) cell viability measured with CellTiter-Blue®. Duration = 24.0 h; cells per well = 80,000 cells/well; Ln^{3+} treatment volume per well = 100 μL; negative control = untreated cells; positive control = only medium without cells to eliminate luminescence/fluorescence background. The X-axis is on a 10^{x} scale. Each data point represents a mean of at least two independent experiments ($n \geq 4$), and error bars show one standard deviation. (For interpretation of the references to color in this figure legend, the reader is referred to the web version of this article.)

reduction is attributed to lanthanide toxicity only. The half-maximum concentration that evoked 50% decrease in I-ATP followed a trend of La^{3+} (794.0 μM) > Lu^{3+} (1115.6 μM) > Gd^{3+} (1488.8 μM) ~ Ce^{3+} (1505.8 μM), as seen in Table 1.

3.3. Cell viability

We further investigated the observed ATP decrease using a cell viability assay, CellTiter-Blue® (CTB), with HepG2 cells. The resazurin assay depends on the metabolic state of treated cells to determine cell viability. Respiring cells reduce CTB (resazurin dye) to a colored form—resorufin. Some cell viability dyes either block electron flow like NADPH (e.g. tetrazolium) or accept electrons like cytochrome; the former dyes are inherently toxic due to electron blockage (McMillian et al., 2002). Like cytochrome oxidase, CTB dye accepts an electron for oxidoreductase as oxygen in the last step of the respiratory chain. Accepting an electron at the final stage of the chain makes CTB less toxic to cell metabolism; thus, it is suitable for cell viability studies. Resazurin reduction involves the loss of an oxygen atom and gain of a hydrogen atom in the resazurin molecule (Fig. S4). This process primarily occurs in the cytoplasm, after which the reduced resazurin is excreted back into the medium (O'Brien et al., 2000). The reduced product, resorufin (pink in color) can be measured both colorimetrically and fluorometrically.

The fluorescence levels of resorufin were measured at 560/590 nm (excitation/emission). All four individual lanthanide compounds showed a dose-dependent increase in cytotoxicity after 24 h of exposure. The average values for cell viability of the negative (no lanthanide treatment) and no-cell control (no HepG2 cells added) were 106.3 ± 12.5% and 1.4 ± 1.6%, respectively. To ensure that the toxicity was from lanthanides and not chloride ions, sodium chloride was tested as a control covering the span of chloride concentration matching to the lanthanide concentration. Fig. 2B shows that chloride ions did not show a significant cytotoxic effect until 15,000 μM (79.6 ± 2.5%).

La and Lu showed the highest cytotoxicity; at 250 μmol-Ln^{3+}/L, cell viability had decreased to less than 80%. After 24 h exposure of HepG2 cells, the EC_{50} values for the tested REEs were between 900 μmol-Ln^{3+}/L and 2900 μmol-Ln^{3+}/L. Cytotoxicity did not correlate with molecular weight. Heavy lanthanides (Lu) showed the highest toxicity, EC_{50} = 951 μmol-Ln^{3+}/L, followed by the light lanthanides (La), EC_{50} = 1249 μmol-Ln^{3+}/L. Both Ce and Gd elicited the least toxicity on the HepG2 cell-line; the EC_{50} toxicity values were 2831 and 2882 μmol-Ln^{3+}/L, respectively. We assume that Ln^{3+} concentration homeostasis is maintained through Ca^{2+} signaling owing to the similarity in structure. The maintenance of Ln^{3+} in cytosol involves active pumping against the gradient by Ca^{2+}-ATPases and cytosolic enzymes. The pumping of Ln^{3+}/Ca^{2+} out of the cytosol against a concentration gradient or by ion exchangers (Na^{+}/Ca^{2+}) is a high energy task (Ghibelli et al., 2010; Szabadkai and Duchen, 2008). Failure to supply sufficient ATP due to long-term exposure inhibits the pumping of Ln^{3+}/Ca^{2+} against the concentration gradient from the cytosol to the endoplasmic reticulum or extracellular environment (Humeau et al., 2018), which causes Ln^{3+}/Ca^{2+} overload. Ln^{3+}/Ca^{2+} overload can be inhibited by the intervention of mitochondria that takes up excess Ln^{3+} from the cytosol; however, the presence of Ln^{3+} that exceeds the physiological threshold causes cell stress and eventually cell death (Ghibelli et al., 2010). In this study, at 5000 μmol-Ln^{3+}/L and below (1.5 h incubation), lanthanides proliferated $\Delta\psi m$; however, a 24-h assessment of I-ATP and cell viability followed a reverse trend. Thus, we hypothesize that the amelioration of $\Delta\psi m$ is short-lived—as the cell runs out of ATP to pump out excess lanthanides, Δp and $\Delta\psi m$ are lost, fostering cell death (Perry et al., 2011; Szabadkai and Duchen, 2008; Tan et al., 2017). In addition, Ln^{3+} has a high affinity for phosphate; the formation of a lanthanide-phosphate bond attenuates the phosphorylation process (Tian et al., 2015), depriving the cell of the energy needed to pump out Ln^{3+}.

When comparing Lu toxicity (EC_{50} = 951 μmol-Ln^{3+}/L) with aluminum towards cell viability, Lu exhibit lower toxicity. At 500 μM, aluminum was responsible for over 50% cell death after 24 h of treatment (Griffioen et al., 2004). Aluminum maltolate induces oxidative stress through structural damage to mitochondria or by inhibiting mitochondrial respiration (Kumar and Gill, 2014). Iron-based coagulants (e.g., ferric chloride) showed a diverse range of cytotoxic effects from potent to mild. At 40 μM, iron can decrease oligodendrocyte cell viability by 50% (Zhang et al., 2005). Using HeLa and HeK 293 cell lines, the toxicity of iron was not pronounced; at 25,000 μM, up to 30% of cells were lost after 24 h of treatment (Shukla et al., 2015). Keeping changes in cell line constant, iron toxicity is driven by the ability of the compound to release iron ions which could explain the deviation. Overall, lanthanides seem to have a mild effect on cell death.

3.4. Chronic toxicity of lanthanides

To assess the chronic (long-term) toxic effect of lanthanides, we used the 72 h CHO cytotoxicity assay (Plewa et al., 2002). Estimating the chronic cytotoxic effect of a xenobiotic using an in vitro assay is challenging due to the nature of the experimental design. This assay exposes the cells to a longer period (72 h) that equals three cell divisions. Therefore, it is able to capture not only cell cytotoxicity but also other changes that might lead to variations of cell proliferation rate or growth inhibition without causing cell death. Chronic toxicity occurs because of repeated or continuous exposure to a contaminant. When cells are exposed to a chemical for a prolonged period, necrosis can occur; otherwise, cells will adjust to the new environment and reproduce/grow. Dead cells cleave from the surface, leaving the live cells to attach. This property can be used to detect cell increase and/or decrease, and if cells are exposed to contaminants for a prolonged period, chronic toxicity can also be estimated. Dyes like tetrazolium and crystal violet (CV) are known to stain live cells. CV binds and stains negatively charged molecules (e.g. protein and DNA) and the extracellular matrix of polysaccharides (Xu et al., 2016). Therefore, when CV is added to a cell culture, viable cells are stained, and the strength of retained CV reflects the number of viable cells. This assay provides a faster analysis of chemotherapeutic compounds that can inhibit cell growth. Cell chronic toxicity has been studied previously with CHO cells (Attene-Ramos et al., 2006; Wang et al., 2011), and this assay has been effectively used to study disinfection byproducts—a major concern in water treatment (Plewa et al., 2004).

Lanthanide exposure did not show strong cytotoxic effects. After three cell cycles (72 h), the cell viability of CHO cells was unaffected up to 2000 μmol-Ln^{3+}/L, after which the cell viability plummeted regardless of the lanthanide ion; chloride concentration did not affect lanthanide toxicity (Fig. 3). The EC_{50} values for the compounds were in the same range, extending from 2096 μM (Ce) to 2543 μM (Gd), Table 1. The chronic potency of lanthanides follows a gradient of Ce ~ Lu > La ~ Gd

Table 1
Lanthanide concentration that induces $EC_{1.5}$ and EC_{50} for I-ATP, cell viability, and chronic toxicity.

Target	Chemical	$EC_{1.5}$ (μM)	EC_{50} (μM)	$R^{2\Delta}$
Intracellular ATP	La^{3+}	241.2	794.0	0.965
	Ce^{3+}	457.7	1505	0.966
	Gd^{3+}	837.7	1488	0.990
	Lu^{3+}	39.9	1115	0.959
Cell viability	La^{3+}	169.9	1249	1.000
	Ce^{3+}	657.5	2831	0.978
	Gd^{3+}	833.1	2882	0.999
	Lu^{3+}	77.23	951.0	0.951
Chronic toxicity	La^{3+}	2318	2415	0.984
	Ce^{3+}	1990	2096	0.983
	Gd^{3+}	2400	2543	0.993
	Lu^{3+}	1883	2197	0.935

$^{\Delta}$ Data is significant at $\rho < 0.05$.

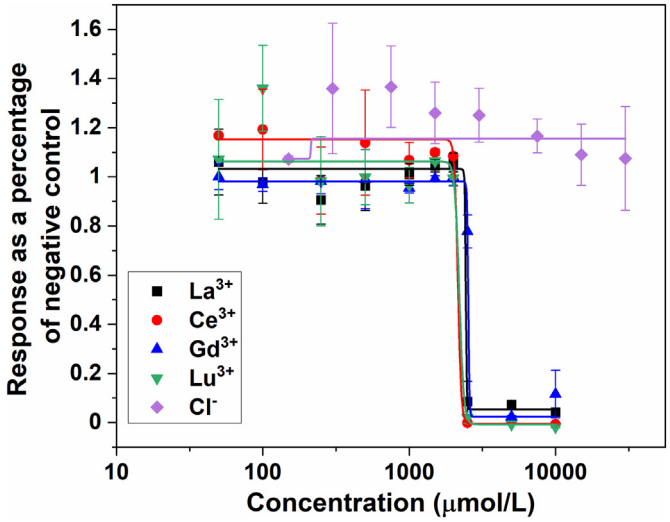

Fig. 3. Chronic toxicity of lanthanides with CHO cells. Exposure duration = 72 h (three cell cycle); cells per well = 3000 cells/well; volume per well = 100 μL; negative control = untreated cells; positive control = only medium without cells to eliminate background fluorescence. X-axis is on $10^{\times}$ scale. Each data point represents a mean of at least two independent experiments ($n \geq 4$), and error bars show one standard deviation.

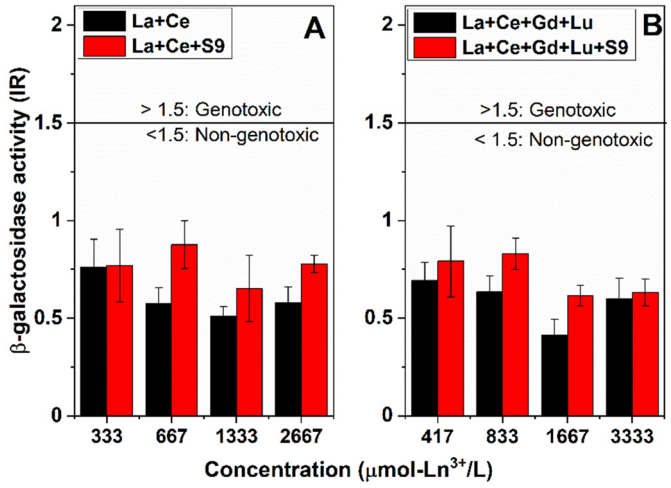

Fig. 4. UmuC assay results. Effect of (A) La + Ce and (B) La + Ce + Gd + Lu mixture on genotoxicity (given as induction ratio, IR) and the growth factor of *S. typhimurium* TA1535/pSK1002 (with and without S9 metabolic activation). Concentrations represent total group concentration, not individual concentrations. The error bars display the standard deviation of 3 replicates. None of the tested mixtures of lanthanides were genotoxic at the tested concentrations.

(Fig. 3). However, based on statistical significance at $\rho = 0.05$, lanthanides elicited similar chronic toxicity. Given a non-acute toxicity exposure (less than 2000 μmol-Ln^{3+}/L), cells are expected to recuperate from lanthanide contamination. Otherwise, there will be a total collapse of $\Delta\psi m$ and/or Δp, triggering cell death as discussed in Section 3.3.

3.5. Genotoxicity of lanthanides

The genotoxicity of lanthanides was assessed using the umuC assay. The umuC assay was first developed in 1985 (Oda et al., 1985), and it is widely used for indirect detection of genotoxicity through DNA damage that triggers the cellular SOS response (Boutry et al., 2013). The assay uses a genetically modified *Salmonella typhimurium* bacteria TA1535/pSK1002 to produce β-galactosidase, which causes a yellow color when the chromogenic substrate is broken down. The extent of β-galactosidase produced and conversion of *o*-nitrophenyl-β-D-galactopyranoside to *o*-nitrophenyl is measured by absorbance (Fig. S5). To evaluate if lanthanides require metabolic activation to become genotoxic, the tests were completed with and without S9 rat liver extract. Most of the available commercial brands of lanthanide coagulants are presented as a mixture with the lighter subclass contributing the largest percentage. Thus, genotoxicity studies were based on light lanthanide subclass (La + Ce) and lanthanides as a whole family (La + Ce + Gd + Lu).

Genotoxicity response in the umuC assay was defined as the induction ratio (IR), which is the ratio of the β-galactosidase activity to growth factor that is inducing an IR of 1.5 ($EC_{IR1.5}$). The growth factor is the response of bacteria treated with lanthanides compared to the negative control (untreated bacteria). Based on the manufacturer's protocol (UMU-ChromoTest ™), a compound that induces $EC_{IR1.5} < 1.5$ is nongenotoxic while $EC_{IR1.5} \geq 1.5$ is genotoxic. The $EC_{IR1.5}$ in the umuC assay were expressed as 4-nitroquinoline-oxide (4NQO) equivalent concentrations for the assay without metabolic activation (—S9) and 2-aminoanthracene (2-AA) equivalent concentrations for the assay with metabolic activation (+S9). Lanthanide mixtures did not induce SOS response as shown in Fig. 4. In addition, lanthanides did not show genotoxicity with metabolic activation (+S9) as the induction ratios were comparable to that of —S9. Therefore, biotransformation of lanthanides, if any, does not affect lanthanide toxicity. Our study agrees with previously published in vitro studies where lanthanum showed no sign of genotoxicity (Damment et al., 2005; Yang et al., 2016). Between 0.2 and 1.2 μg/mL, ferric chloride enhanced mutant frequency lymphoma cells with +S9; however, without S9, there was barely any toxicity (Dunkel et al., 1999). Therefore, lanthanides are potentially a better alternative in water treatment since their toxicity is not increased by biotransformation. To the best of our knowledge, this is the first time that the genotoxicity of soluble lutetium is reported.

3.6. Additivity, antagonistic and synergistic (AAS) effect of lanthanides

Contaminants in the water system can exist as a single compound or as a group. Studying a mixture response offers a quick approach to determine the combined effect of chemicals, which is often not assessed in laboratory trials, or response additivity is wrongly assumed for chemicals of a similar nature. We studied the AAS of lanthanides at different combinations to establish the CI using the CT model for chronic toxicity, I-ATP, and cell viability. Upon fitting individual dose-response curves, the median-effect equation (Eq. 3) was applied to generate the fraction of affected cells and I-ATP.

$$f_a = 1/[1 + (D_m/D)^m] \quad (3)$$

Here, f_a represents the fraction of affected cells/I-ATP, D_m is the median-effect dose, D is the dose, and m is the slope. The resulting parameters were used to calculate CI. At $CI < 0.9$, $0.9 \leq CI \leq 1.10$, and $CI > 1.1$, the nature of AAS are synergistic, additive, and antagonistic, respectively (Chou, 2010; Rider and Simmons, 2018). Table 2 summarizes the different CI values and f_a for various lanthanide combinations that were investigated (Fig. S6). At 1000 μmol-Ln^{3+}/L and below, all the combinations showed an antagonistic behavior towards I-ATP depletion. I-ATP was reduced more by the light lanthanide combination (La + Ce) compared to La + Ce + Gd + Lu mixture. A similar trend was observed for cell viability using CTB. The addition of heavy subclasses into the light subclass increased the chronic toxicity of the lanthanides family. At an individual level, Lu (heavy) was more potent at inducing chronic toxicity compared to other lanthanides. Thus, the toxicity of lanthanides is driven by heavy lanthanides. However, the overall toxicity of the mixtures was less pronounced compared to individual compounds at the same concentration. For example, at 4000 μmol-Ln^{3+}/L, individual lanthanides reduced the percentage of viable cells to less than 50%, while the combination of four compounds affected, at

Table 2
Assessment of CI values at different lanthanide doses (μM) and combinations.

	Light (La + Ce)			La + Ce + Gd + Lu		
	Total dose (μmol-Ln^{3+}/L) ⁑	f_a	**CI Value**	**Total dose (μmol-Ln^{3+}/L)** ⁑	f_a	**CI Value**
I-ATP	100	0.025	4.516	100	0.001	416.1
	500	0.025	22.58	500	0.03	18.77
	1000	0.161	2.742	1000	0.045	21.15
	2500	0.782	0.121	2500	0.752	0.188
	4000	0.789	0.183	4000	0.922	0.048
Viability	100	0.029	17.65	100	0.023	28.13
	500	0.001	12890	500	0.001	13919
	1000	0.034	138.7	1000	0.035	150.1
	2500	0.376	5.444	2500	0.407	5.264
	4000	0.383	8.340	4000	0.383	9.742
Chronic	100	0.001	870.8	100	0.001	20155
	500	0.001	4354	500	0.011	72.67
	1000	0.001	8708	1000	0.084	1.874
	2000	0.003	13.45	2000	0.277	0.381
	2500	0.072	3.029	2500	0.527	0.092

f_a: Fraction affected; CI: Combination index; Highlighted rows indicate the change from antagonism to synergism for the respective mixture and assay. ⁑For a given combination dose, the molar ratio was 1:1.

most 40% cells ($f_a = 38.3\%$). Given their physical and chemical similarities, we hypothesize that lanthanides compete for the same sites, which reduces their toxicity potency—hence showing antagonistic behavior. Therefore, a mixture of REEs in water treatment would be preferential as the overall biological effect is less than additive.

Tan et al. (2017) observed the AAS behavior of lanthanides during algae growth; the presence of different REE compounds decreased their combined toxicity. While assessing the effect of lanthanide mixtures on seven aquatic biotas, Romero-Freire et al. (2019) observed both synergistic and antagonistic behavior of lanthanides. The antagonistic and synergistic observations can be related to a combination of stress factors (Liess et al., 2016), and/or phosphate precipitation due to high lanthanide affinity. La, Gd, and yttrium showed neither synergistic nor antagonistic characteristics in *Cyprinus carpio* (Qiang et al., 1994; Tai et al., 2010).

4. Conclusion

This study assessed the changes of Δψm, I-ATP, cell viability, chronic cytotoxicity and genotoxicity of lanthanides using HepG2, CHO cell lines, and umuC assay. The toxicity of lanthanides was assessed using Δψm indicator solution, Celltiter-Blue®, Celltiter-Glo®, crystal violet, and umuC assay. At 5000 μmol-Ln^{3+}/L and above, Δψm is completely lost, possibly due to an excessive lanthanide influx that surpasses the mitochondria's ability to shield/pump them out. At low concentrations, the NCX can effectively pump out excess lanthanides; however, this increases Δψm because NCX is an energy-intensive mechanism. When I-ATP was measured as a function of lanthanide concentration, there was a steady decrease in I-ATP between 100 and 4000 μmol-Ln^{3+}/L. Cell viability and chronic toxicity were strongly influenced by heavy REE. In addition, the presence of Lu in the matrix increased necrosis and chronic toxicity. Regardless of the tested assay, at less than 1000 μmol-Ln^{3+}/L, lanthanides exhibited an antagonistic behavior. Thus, in wastewater treatment by coagulation or adsorption processes, using lanthanides as a mixture could weaken their environmental impact. When compared to traditional coagulants like iron and aluminum, lanthanides caused lower effects on Δψm, cell viability and genotoxicity. The lower toxicity of lanthanides could make them a good candidate in wastewater treatment. Cell viability, I-ATP, and chronic toxicity assays were sensitive to lanthanide concentration with I-ATP assay being the most sensitive. Thus, in pursuit of bioanalytical monitoring tools for lanthanides in wastewater effluent or surface waters, the I-ATP assay should be considered and explored as an option.

CRediT authorship contribution statement

George William Kajjumba: Data collection, analysis, Writing-Reviewing, and Editing

Matias Attene-Ramos: Methodology development, Writing-Reviewing and Editing

Erica J. Marti: Writing- Data curation, Reviewing and Editing.

Rachael Bokota: Data curation

Declaration of competing interest

The authors declare that they have no known competing financial interests or personal relationships that could have appeared to influence the work reported in this paper.

Acknowledgement

This research was supported by a National Science Foundation award in the USA (#1833108). Thanks to Rachael Bokota for her assistance during data collection and Dr. Michael Plewa for supplying us with CHO cells.

Appendix A. Supplementary data

Supplementary data to this article can be found online at https://doi.org/10.1016/j.scitotenv.2021.149556.

References

Abbas, T., Kajjumba, G.W., Ejjada, M., Masrura, S.U., Marti, E.J., Khan, E., Jones-lepp, T.L., 2020. Recent advancements in the removal of cyanotoxins from water using conventional and modified adsorbents—a contemporary review. Water (Switzerland) 12, 2756. https://doi.org/10.3390/w12102756.

Aldridge, W.N., Street, B.W., 1964. Oxidative phosphorylation. biochemical effects and properties of trialkyltins. Biochem. J. 91, 287–297. https://doi.org/10.1042/bj0910287.

Arab-Nozari, M., Zamani, E., LAtifi Shaki, A., 2019. Mitochondrial toxicity of aluminium nanoparticles in comparison to its ionic form on isolated rat brain mitochondria. Bratislava Med. J. 120, 516–522. https://doi.org/10.4149/BLL.

Arya, A., Sethy, N.K., Das, M., Singh, S.K., Das, A., Ujjain, S.K., Sharma, R.K., Sharma, M., Bhargava, K., 2014. Cerium oxide nanoparticles prevent apoptosis in primary cortical culture by stabilizing mitochondrial membrane potential. Free Radic. Res. 48, 784–793. https://doi.org/10.3109/10715762.2014.906593.

Attene-Ramos, M.S., Wagner, E.D., Plewa, M.J., Gaskins, H.R., 2006. Evidence that hydrogen sulfide is a genotoxic agent. Mol. Cancer Res. 4, 9–14. https://doi.org/10.1158/1541-7786.MCR-05-0126.

Attene-Ramos, M.S., Huang, R., Michael, S., Witt, K.L., Richard, A., Tice, R.R., Simeonov, A., Austin, C.P., Xia, M., 2015. Profiling of the Tox21 chemical collection for mitochondrial function to identify compounds that acutely decrease mitochondrial membrane potential. Environ. Health Perspect. 123, 49–56. https://doi.org/10.1289/ehp.1408642.

Blinova, I., Lukjanova, A., Muna, M., Vija, H., Kahru, A., 2018. Evaluation of the potential hazard of lanthanides to freshwater microcrustaceans. Sci. Total Environ. 642, 1100–1107. https://doi.org/10.1016/j.scitotenv.2018.06.155.

Boutry, C., Delplace, B., Clippe, A., Fontaine, L., Hols, P., 2013. SOS response activation and competence development are antagonistic mechanisms in Streptococcus thermophilus. J. Bacteriol. 195, 696–707. https://doi.org/10.1128/JB.01605-12.

Chou, T.C., 2010. Drug combination studies and their synergy quantification using the chou-talalay method. Cancer Res. https://doi.org/10.1158/0008-5472.CAN-09-1947.

Damment, S.J.P., Beevers, C., Gatehouse, D.G., 2005. Evaluation of the potential genotoxicity of the phosphate binder lanthanum carbonate. Mutagenesis 20, 29–37. https://doi.org/10.1093/mutage/gei003.

Duchen, M.R., 2004. Mitochondria in health and disease: perspectives on a new mitochondrial biology. Mol. Asp. Med. https://doi.org/10.1016/j.mam.2004.03.001.

Dunkel, V.C., San, R.H.C., Seifried, H.E., Whittaker, P., 1999. Genotoxicity of iron compounds in salmonella typhimurium and L5178Y mouse lymphoma cells. Environ. Mol. Mutagen. 33, 28–41. https://doi.org/10.1002/(SICI)1098-2280(1999)33:1<28::AID-EM4>3.0.CO;2-S.

Feyerabend, F., Fischer, J., Holtz, J., Witte, F., Willumeit, R., Drücker, H., Vogt, C., Hort, N., 2010. Evaluation of short-term effects of rare earth and other elements used in magnesium alloys on primary cells and cell lines. Acta Biomater. 6, 1834–1842. https://doi.org/10.1016/j.actbio.2009.09.024.

Ghibelli, L., Cerella, C., Diederich, M., 2010. The dual role of calcium as messenger and stressor in cell damage, death, and survival. Int. J. Cell Biol. https://doi.org/10.1155/2010/546163.

Griffioen, K.J.S., Ghribi, O., Fox, N., Savory, J., Dewitt, D.A., 2004. Aluminum maltolate-induced toxicity in NT2 cells occurs through apoptosis and includes cytochrome c release. Neurotoxicology 25, 859–867. https://doi.org/10.1016/j.neuro.2003.12.004.

Hannah, R., Beck, M., Moravec, R., Riss, T., 2001. Cell titer-GloTM luminescent cell viability assay: a sensitive and rapid method for determining cell viability. Promega Cell Notes 2, 11–13.

Herrmann, H., Nolde, J., Berger, S., Heise, S., 2016. Aquatic ecotoxicity of lanthanum - a review and an attempt to derive water and sediment quality criteria. Ecotoxicol. Environ. Saf. https://doi.org/10.1016/j.ecoenv.2015.09.033.

Huang, R., Southall, N., Cho, M.H., Xia, M., Inglese, J., Austin, C.P., 2008. Characterization of diversity in toxicity mechanism using in vitro cytotoxicity assays in quantitative high throughput screening. Chem. Res. Toxicol. 21, 659–667. https://doi.org/10.1021/tx700365e.

Humeau, J., Bravo-San Pedro, J.M., Vitale, I., Nuñez, L., Villalobos, C., Kroemer, G., Senovilla, L., 2018. Calcium signaling and cell cycle: progression or death. Cell Calcium https://doi.org/10.1016/j.ceca.2017.07.006.

Hussain, S., Al-Nsour, F., Rice, A.B., Marshburn, J., Yingling, B., Ji, Z., Zink, J.I., Walker, N.J., Garantziotis, S., 2012. Cerium dioxide nanoparticles induce apoptosis and autophagy in human peripheral blood monocytes. ACS Nano 6, 5820–5829. https://doi.org/10.1021/nn302235u.

Hussain, S., Kodavanti, P.P., Marshburn, J.D., Janoshazi, A., Marinakos, S.M., George, M., Rice, A., Wiesner, M.R., Garantziotis, S., 2016. Decreased uptake and enhanced mitochondrial protection underlie reduced toxicity of nanoceria in human monocyte-derived macrophages. J. Biomed. Nanotechnol. 12, 2139–2150. https://doi.org/10.1166/jbn.2016.2320.

Islami-Moghaddam, M., Mansouri-Torshizi, H., Divsalar, A., Saboury, A.A., 2009. Synthesis, characterization, cytotoxic and DNA binding studies of diimine Platinum(II) and Palladium(II) complexes of short hydrocarbon chain ethyldithiocarbamate ligand. J. Iran. Chem. Soc. 6, 552–569. https://doi.org/10.1007/BF03246535.

Kajjumba, G.W., Fischer, D., Risso, L., Koury, D., Marti, E.J., 2021. Application of cerium and lanthanum coagulants in wastewater treatment—a comparative assessment to magnesium, aluminum, and iron coagulants. Chem. Eng. J. 131268. https://doi.org/10.1016/j.cej.2021.131268.

Kumar, V., Gill, K.D., 2014. Oxidative stress and mitochondrial dysfunction in aluminium neurotoxicity and its amelioration: a review. Neurotoxicology https://doi.org/10.1016/j.neuro.2014.02.004.

Lesnefsky, E.J., Moghaddas, S., Tandler, B., Kerner, J., Hoppel, C.L., 2001. Mitochondrial dysfunction in cardiac disease: ischemia - reperfusion, aging, and heart failure. J. Mol. Cell. Cardiol. https://doi.org/10.1006/jmcc.2001.1378.

Liess, M., Foit, K., Knillmann, S., Schäfer, R.B., Liess, H.D., 2016. Predicting the synergy of multiple stress effects. Sci. Rep. 6, 1–8. https://doi.org/10.1038/srep32965.

McMillian, M.K., Li, L., Parker, J.B., Patel, L., Zhong, Z., Gunnett, J.W., Powers, W.J., Johnson, M.D., 2002. An improved resazurin-based cytotoxicity assay for hepatic cells. Cell Biol. Toxicol. 18, 157–173. https://doi.org/10.1023/A:1015559603643.

Mitchell, P., Moyle, J., 1969. Estimation of membrane potential and pH difference across the cristae membrane of rat liver mitochondria. Eur. J. Biochem. 7, 471–484. https://doi.org/10.1111/j.1432-1033.1969.tb19633.x.

Nicholls, D.G., Budd, S.L., 2000. Mitochondria and neuronal survival. Physiol. Rev. https://doi.org/10.1152/physrev.2000.80.1.315.

O'Brien, J., Wilson, I., Orton, T., Pognan, F., 2000. Investigation of the alamar blue (resazurin) fluorescent dye for the assessment of mammalian cell cytotoxicity. Eur. J. Biochem. 267, 5421–5426. https://doi.org/10.1046/j.1432-1327.2000.01606.x.

Oda, Y., Nakamura, S.ichi, Oki, I., Kato, T., Shinagawa, H., 1985. Evaluation of the new system (umu-test) for the detection of environmental mutagens and carcinogens. Mutat. Res. Mutagen. Relat. Subj. 147, 219–229. https://doi.org/10.1016/0165-1161(85)90062-7.

Pagano, G., Aliberti, F., Guida, M., Oral, R., Siciliano, A., Trifuoggi, M., Tommasi, F., 2015. Rare earth elements in human and animal health: state of art and research priorities. Environ. Res. https://doi.org/10.1016/j.envres.2015.06.039.

Parsons, J.T., 2003. Focal adhesion kinase: the first ten years. J. Cell Sci. 116, 1409–1416. https://doi.org/10.1242/jcs.00373.

Perry, S.W., Norman, J.P., Barbieri, J., Brown, E.B., Gelbard, H.A., 2011. Mitochondrial membrane potential probes and the proton gradient: a practical usage guide. Biotechniques https://doi.org/10.2144/000113610.

Pieczenik, S.R., Neustadt, J., 2007. Mitochondrial dysfunction and molecular pathways of disease. Exp. Mol. Pathol. 83, 84–92. https://doi.org/10.1016/j.yexmp.2006.09.008.

Plewa, M.J., Kargalioglu, Y., Vankerk, D., Minear, R.A., Wagner, E.D., 2002. Mammalian cell cytotoxicity and genotoxicity analysis of drinking water disinfection by-products. Environ. Mol. Mutagen. 40, 134–142. https://doi.org/10.1002/em.10092.

Plewa, M.J., Wagner, E.D., Jazwierska, P., Richardson, S.D., Chen, P.H., McKague, A.B., 2004. Halonitromethane drinking water disinfection byproducts: chemical characterization and mammalian cell cytotoxicity and genotoxicity. Environ. Sci. Technol. 38, 62–68. https://doi.org/10.1021/es030477l.

Plewa, M.J., Simmons, J.E., Richardson, S.D., Wagner, E.D., 2010. Mammalian cell cytotoxicity and genotoxicity of the haloacetic acids, a major class of drinking water disinfection by-products. Environ. Mol. Mutagen. 51, 871–878. https://doi.org/10.1002/em.20585.

Qiang, T., Xiao-rong, W., Li-qing, T., Le-mei, D., 1994. Bioaccumulation of the rare earth elements lanthanum, gadolinium and yttrium in carp (Cyprinus carpio). Environ. Pollut. 85, 345–350. https://doi.org/10.1016/0269-7491(94)90057-4.

R. Kulperger R. Okun G. Munford Methods and compositions using lanthanum for removing phosphates from water US6338800B1. 2001

Recillas, S., García, A., González, E., Casals, E., Puntes, V., Sánchez, A., Font, X., 2012. Preliminary study of phosphate adsorption onto cerium oxide nanoparticles for use in water purification; nanoparticles synthesis and characterization. Water Sci. Technol. 66, 503–509. https://doi.org/10.2166/wst.2012.185.

Reeves, J.P., Condrescu, M., 2003. Lanthanum is transported by the sodium/calcium exchanger and regulates its activity. Am. J. Physiol. - Cell Physiol. 285. https://doi.org/10.1152/ajpcell.00168.2003.

Rider, C.V., Simmons, J.E., 2018. Chemical Mixtures and Combined Chemical and Nonchemical Stressors: Exposure, Toxicity, Analysis, and Risk. 1st ed. Springer Nature, Cham https://doi.org/10.1007/978-3-319-56234.

Riss, T., O'Brien, M., Moravec, R., 2003. Choosing the right cell-based assay for your research. Cell Notes 6–12. https://doi.org/10.1200/JCO.2011.36.1360.

Romero-Freire, A., Joonas, E., Muna, M., Cossu-Leguille, C., Vignati, D.A.L., Giamberini, L., 2019. Assessment of the toxic effects of mixtures of three lanthanides (Ce, gd, Lu) to aquatic biota. Sci. Total Environ. 661, 276–284. https://doi.org/10.1016/j.scitotenv.2019.01.155.

Sakamuru, S., Attene-Ramos, M.S., Xia, M., 2016. Mitochondrial membrane potential assay. Methods Mol. Biol. 1473, 17–22. https://doi.org/10.1007/978-1-4939-6346-1_2.

Shen, C., Zhang, G., Meng, Q., 2012. Regulation of epithelial cell morphology and functions approaching to more in vivo-like by modifying polyethylene glycol on polysulfone membranes. PLoS One 7, e36110. https://doi.org/10.1371/journal.pone.0036110.

Shukla, S., Jadaun, A., Arora, V., Sinha, R.K., Biyani, N., Jain, V.K., 2015. In vitro toxicity assessment of chitosan oligosaccharide coated iron oxide nanoparticles. Toxicol. Rep. 2, 27–39. https://doi.org/10.1016/j.toxrep.2014.11.002.

Slack, J.K., Adams, R.B., Rovin, J.D., Bissonette, E.A., Stoker, C.E., Parsons, J.T., 2001. Alterations in the focal adhesion kinase/Src signal transduction pathway correlate with increased migratory capacity of prostate carcinoma cells. Oncogene 20, 1152–1163. https://doi.org/10.1038/sj.onc.1204208.

Szabadkai, G., Duchen, M.R., 2008. Mitochondria: the hub of cellular Ca2+ signaling. Physiology https://doi.org/10.1152/physiol.00046.2007.

Tai, P., Zhao, Q., Su, D., Li, P., Stagnitti, F., 2010. Biological toxicity of lanthanide elements on algae. Chemosphere 80, 1031–1035. https://doi.org/10.1016/j.chemosphere.2010.05.030.

Tan, Q.G., Yang, G., Wilkinson, K.J., 2017. Biotic ligand model explains the effects of competition but not complexation for sm biouptake by Chlamydomonas reinhardtii. Chemosphere 168, 426–434. https://doi.org/10.1016/j.chemosphere.2016.10.051.

Tian, J., Zeng, X., Xie, X., Han, S., Liew, O.W., Chen, Y.T., Wang, L., Liu, X., 2015. Intracellular adenosine triphosphate deprivation through lanthanide-doped nanoparticles. J. Am. Chem. Soc. 137, 6550–6558. https://doi.org/10.1021/jacs.5b00981.

Tomasello, L., Cluts, L., Croce, C.M., 2019. Experimental validation of MicroRNA targets: luciferase reporter assay. Methods Mol. Biol., 315–330 https://doi.org/10.1007/978-1-4939-9207-2_17.

Wang, S., Hunter, L.A., Arslan, Z., Wilkerson, M.G., Wickliffe, J.K., 2011. Chronic exposure to nanosized, anatase titanium dioxide is not cyto- or genotoxic to chinese hamster ovary cells. Environ. Mol. Mutagen. 52, 614–622. https://doi.org/10.1002/em.20660.

Wang, Z., Shen, D., Shen, F., Li, T., 2016. Phosphate adsorption on lanthanum loaded biochar. Chemosphere 150, 1–7. https://doi.org/10.1016/j.chemosphere.2016.02.004.

Weltje, L., Heidenreich, H., Zhu, W., Wolterbeek, H.T., Korhammer, S., Goeij, J.J.M., Markert, B., 2002. Lanthanide concentrations in freshwater plants and molluscs, related to those in surface water, pore water and sediment. a case study in the Netherlands. Sci. Total Environ. 286, 191–214. https://doi.org/10.1016/S0048-9697(01)00978-0.

Wu, J., Yang, J., Liu, Q., Wu, S., Ma, H., Cai, Y., 2013. Lanthanum induced primary neuronal apoptosis through mitochondrial dysfunction modulated by Ca2+ and Bcl-2 family. Biol. Trace Elem. Res. 152, 125–134. https://doi.org/10.1007/s12011-013-9601-3.

Xu, Z., Liang, Y., Lin, S., Chen, D., Li, B., Li, L., Deng, Y., 2016. Crystal violet and XTT assays on Staphylococcus aureus biofilm quantification. Curr. Microbiol. 73, 474–482. https://doi.org/10.1007/s00284-016-1081-1.

Yang, H., Zhang, X., Liu, H., Cui, W., Zhang, Q., Li, Y., Yu, Z., Jia, X., 2016. Lanthanum nitrate genotoxicity evaluation: Ames test, mouse micronucleus assay, and chromosome aberration test. Mutat. Res. - Genet. Toxicol. Environ. Mutagen. 810, 1–5. https://doi.org/10.1016/j.mrgentox.2016.09.008.

Zhang, X., Haaf, M., Todorich, B., Grosstephan, E., Schieremberg, H., Surguladze, N., Connor, J.R., 2005. Cytokine toxicity to oligodendrocyte precursors is mediated by iron. Glia 52, 199–208. https://doi.org/10.1002/glia.20235.

Zhang, Y., Fu, L.J., Li, J.X., Yang, X.G., Yang, X.Da., Wang, K., 2009. Gadolinium promoted proliferation and enhanced survival in human cervical carcinoma cells. BioMetals 22, 511–519. https://doi.org/10.1007/s10534-009-9208-5.